Supporting Information for

Perovskite Solar Cells Powered Electrochromic Batteries for Smart Windows

Xinhui Xia, [‡a,*] Zhiliang Ku,[b] Ding Zhou,[a] Yu Zhong,[a] Yongqi Zhang,[c] Yadong Wang,[d] Min Joon Huang,[d] Jiangping Tu,[a,*] Hong Jin Fan[c,*]

[a] *State Key Laboratory of Silicon Materials, Key Laboratory of Advanced Materials and Applications for Batteries of Zhejiang Province, and Department of Materials Science and Engineering, Zhejiang University, Hangzhou 310027, P. R. China. Email: helloxxh@zju.edu.cn; tujp@zju.edu.cn*

[b] *State Key Lab of Advanced Technologies for Materials Synthesis and Processing, Wuhan University of Technology, Wuhan, 430070, P. R. China*

[c] *School of Physical and Mathematical Sciences, Nanyang Technological University, Singapore 637371, Singapore. Email: fanhj@ntu.edu.sg*

[d] *School of Engineering, Nanyang Polytechnic, 569830, Singapore*

[‡] Xinhui Xia and Zhiliang Ku contributed equally.

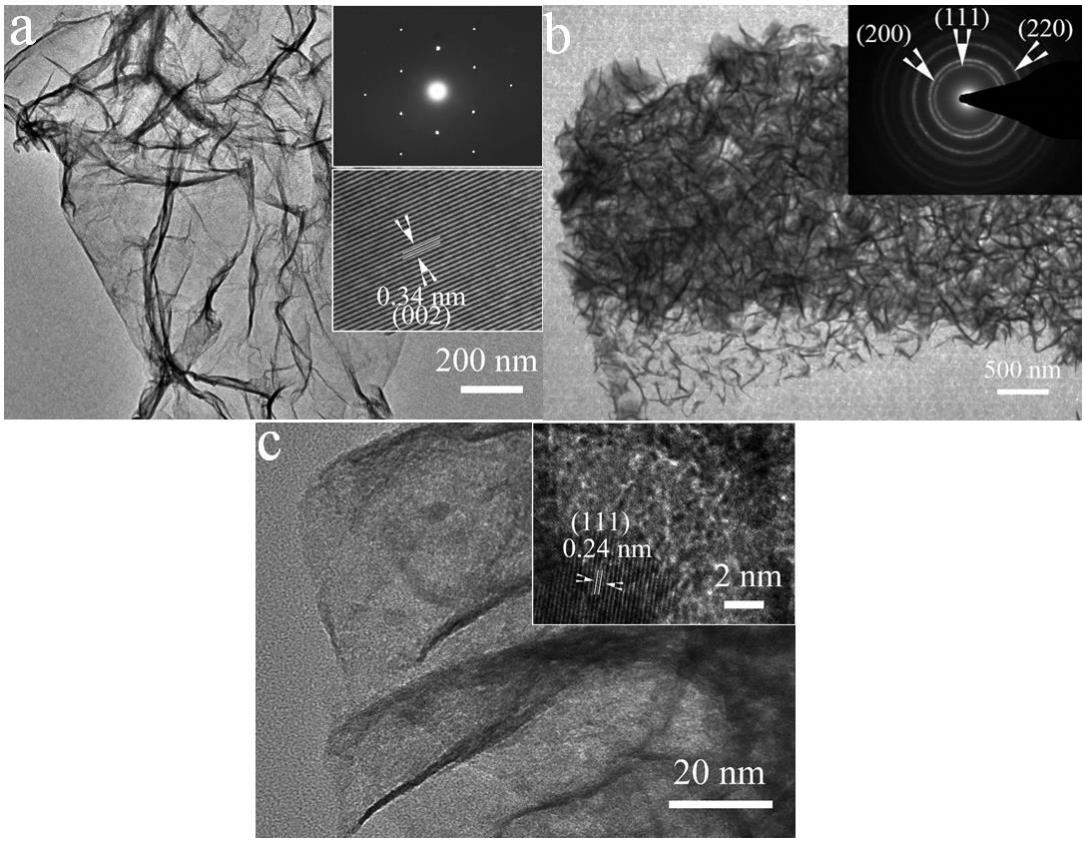

Figure S1. (a) TEM image of rGO sheet (SAED pattern and HRTEM image in insets); (b, c) TEM images of NiO nanoflakes (SAED pattern and HRTEM image in insets).

Description of Figure S1: TEM image (Figure S1 a) shows that the rGO has thin wrinkled sheet appearance and exhibits crystalline selected area electron diffraction (SAED) pattern with typical six-fold symmetry of graphene. The measured interplanar spacing is about 0.34 nm, which corresponds to the (002) planes of graphitic carbon (JCPDS 75-1621). Interconnected thin nanoflakes structure of the NiO is demonstrated by the TEM results in b and c. SAED patterns of the nanoflakes are well indexed to polycrystalline cubic NiO phase (JCPDS 4-0835). The calculated interplanar distance of 0.24 m corresponds to the d-spacing of (111) planes of NiO (JCPDS 4-0835).

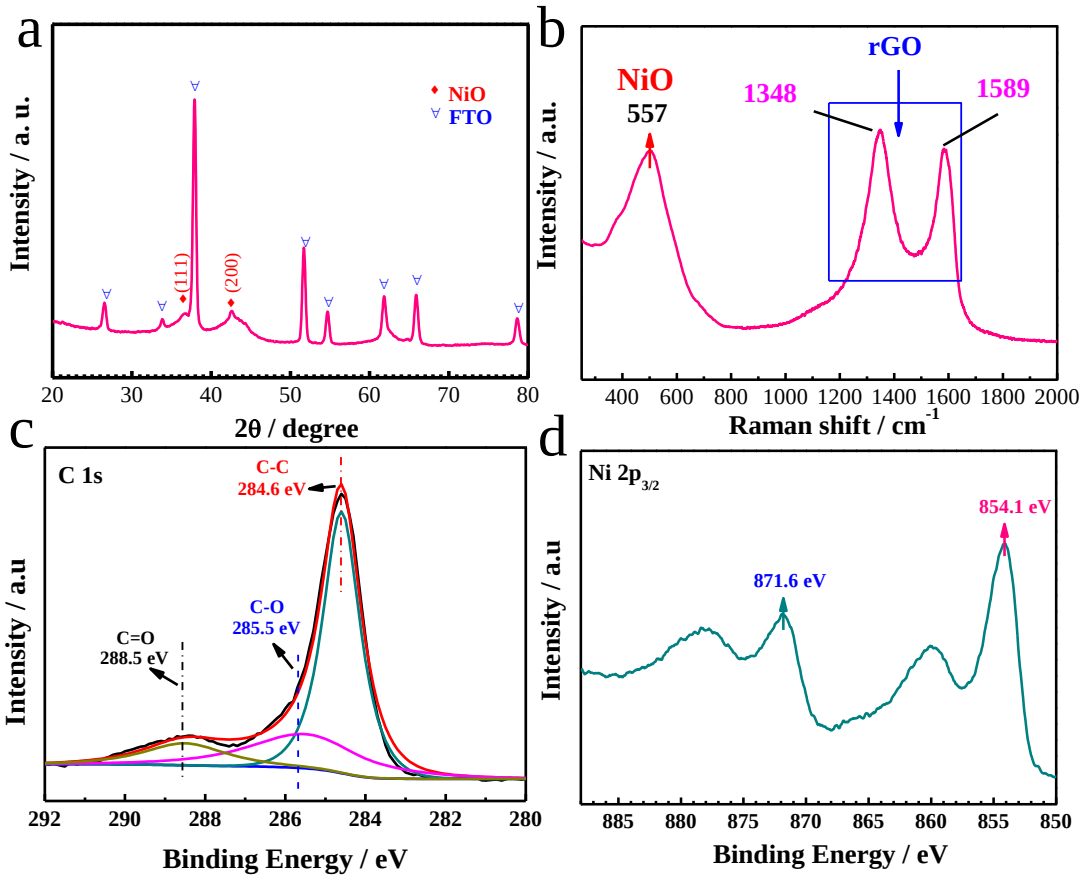

Figure S2. Structural and composition characterizations of the rGO-connected bilayer NiO nanoflakes arrays: (a) XRD pattern on the FTO substrate; (b) Raman spectrum; XPS analysis: (c) C1s spectra and (d) Ni 2p spectra.

Description of Figure S2: In the XRD pattern shown in **Figure S2**a, in addition to the peaks of FTO substrate, two diffraction peaks (111) and (200) of NiO are noticed. No typical peaks of rGO are observed because of its extremely low content in the composite bilayer films. But the presence of rGO and NiO is confirmed by the Raman spectrum (Figure S2b). The Raman peaks at 1348 and 1589 cm^{-1} are characteristic of D-band and G-band of rGO. The peak at 557 cm^{-1} belongs to Ni-O band.[1] Meanwhile, XPS test is further conducted to check the composition of bilayer composite films. For the C 1s specta, there are three peaks at 284.6, 285.5 and 287.5 eV, which are attributed to the C–C, C–O and C=O species, respectively (Figure S2c). As compared to the C-C peak, the peak intensities of C–O and C=O are much lower, indicating that the rGO does not have many functional groups and show good quality. For the Ni 2p spectra, two main core level Ni 2p1/2 (871.6 eV) and Ni 2p3/2 (854 eV) are noticed and the binding energy separation between core levels is about 17.6 eV (Figure S2d), which match well with NiO phase.[2]

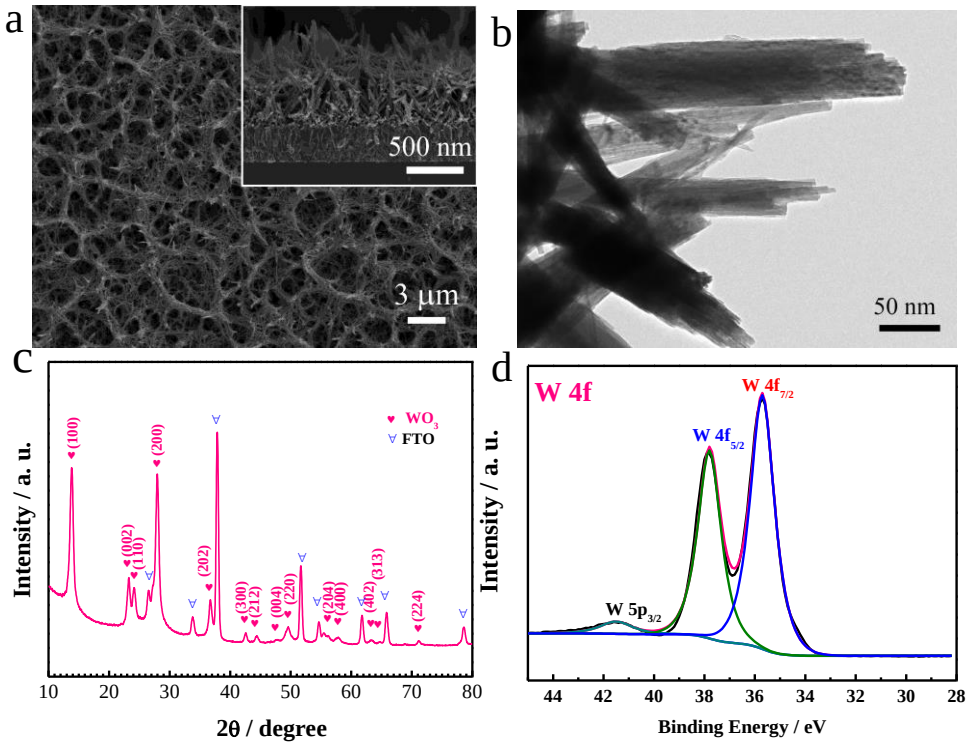

Figure S3. More characterization of the WO_3 nanowires arrays: (a) Low-magnification SEM image; (b) TEM images; (c) XRD pattern on the FTO substrate; (d) XPS spectrum of the W4f peaks.

Description of Figure S3: Except for the diffraction peaks of FTO substrate, the left peaks are well indexed as hexagonal WO_3 phase (JCPDS 85-2459). In the XPS spectrum, three W4f core levels located at 35.6 (W $4f_{7/2}$), 37.6 (W $4f_{5/2}$) and 41.5 eV (W $5p_{3/2}$) are noticed, which match well with electronic states of W^{6+} in WO_3.[3]

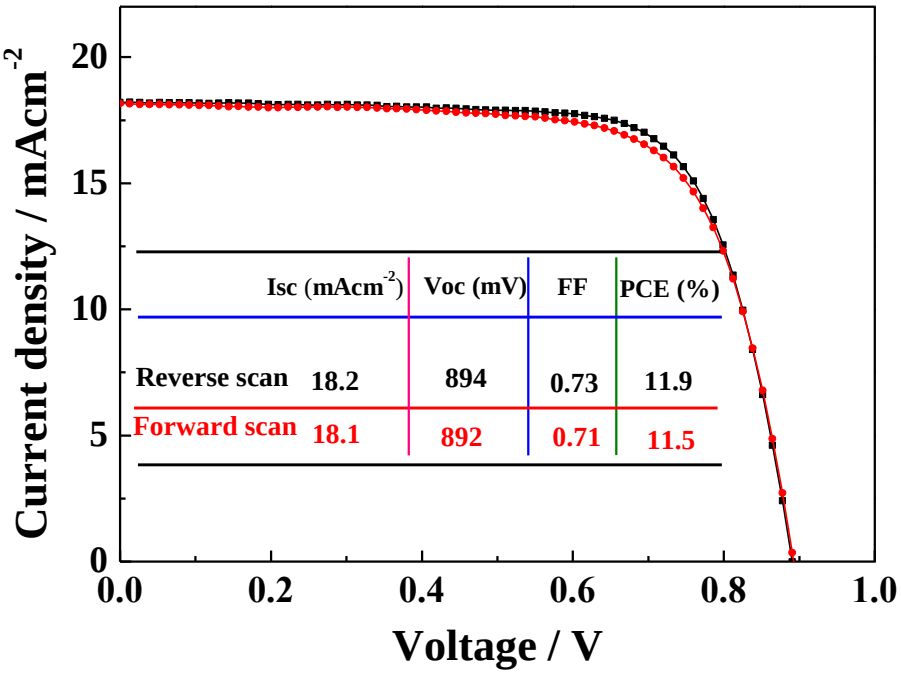

Figure S4. The photocurrent density-voltage characteristics of the carbon-based PSCs device were taken under AM 1.5G standard illumination with a mask of 0.16 cm^2. By scanning from 1 to 0 V (reverse scan), the device presents an V_{oc} of 894 mV, a I_{sc} of 18.2 mA/cm^2, and a FF of 0.73, corresponding to a PCE of 11.9 %. While scanning from 0 V to 1 V (forward scan), the FF of the device has a slight decrease from 0.73 to 0.71, yielding a PCE of 11.5 %.

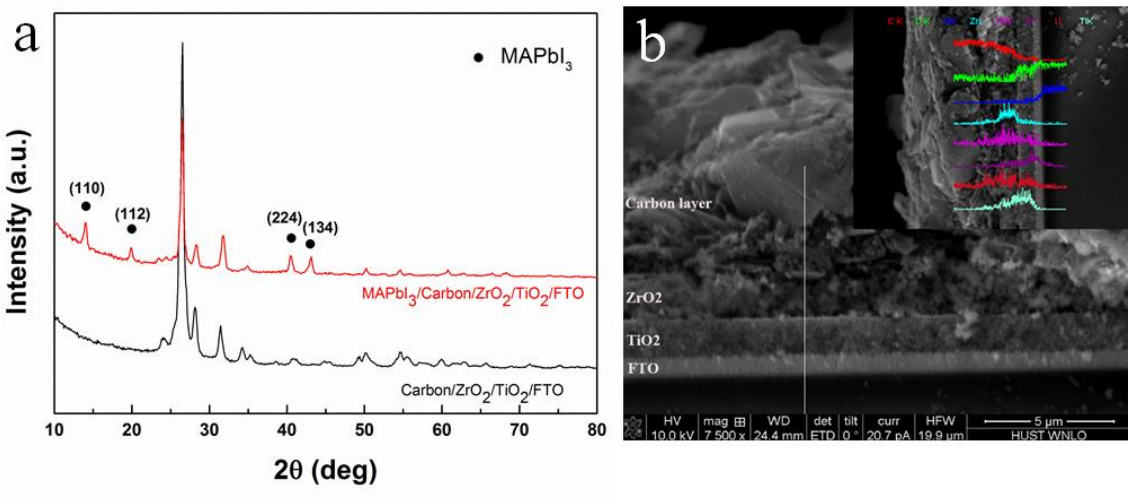

Figure S5 (a) XRD patterns recorded on the perovskite solar cell before (black) and after (red) the filling of $MAPbI_3$ perovskite. (b) SEM image observed from the cross section of the device and EDS analysis scanning along the white line (inset).

Characterization of the perovskite solar cells

The perovskite solar cells have a sandwich structure with the mesoporous TiO_2 layer on the bottom, mesoporous ZrO_2 layer in the middle and mesoporous carbon layer on the top. All these mesoporous layers were filled with $MAPbI_3$ perovskite by the method reported previously (see more details in Ref. 4) By X ray diffraction spectroscopy (XRD), we can clearly find the (110), (112), (224) and (134) peaks of $MAPbI_3$ perovskite crystal at 2θ=14.1°, 19.8°, 40.4° and 43.0°, respectively (see Figure S5a). EDX analysis along the cross section of the device (see SEM image in Figure S5b) confirm the existence of Pb and I elements across all the three layers (TiO_2, ZrO_2 and carbon), indicating a complete filling of $MAPbI_3$ perovskite in the device.

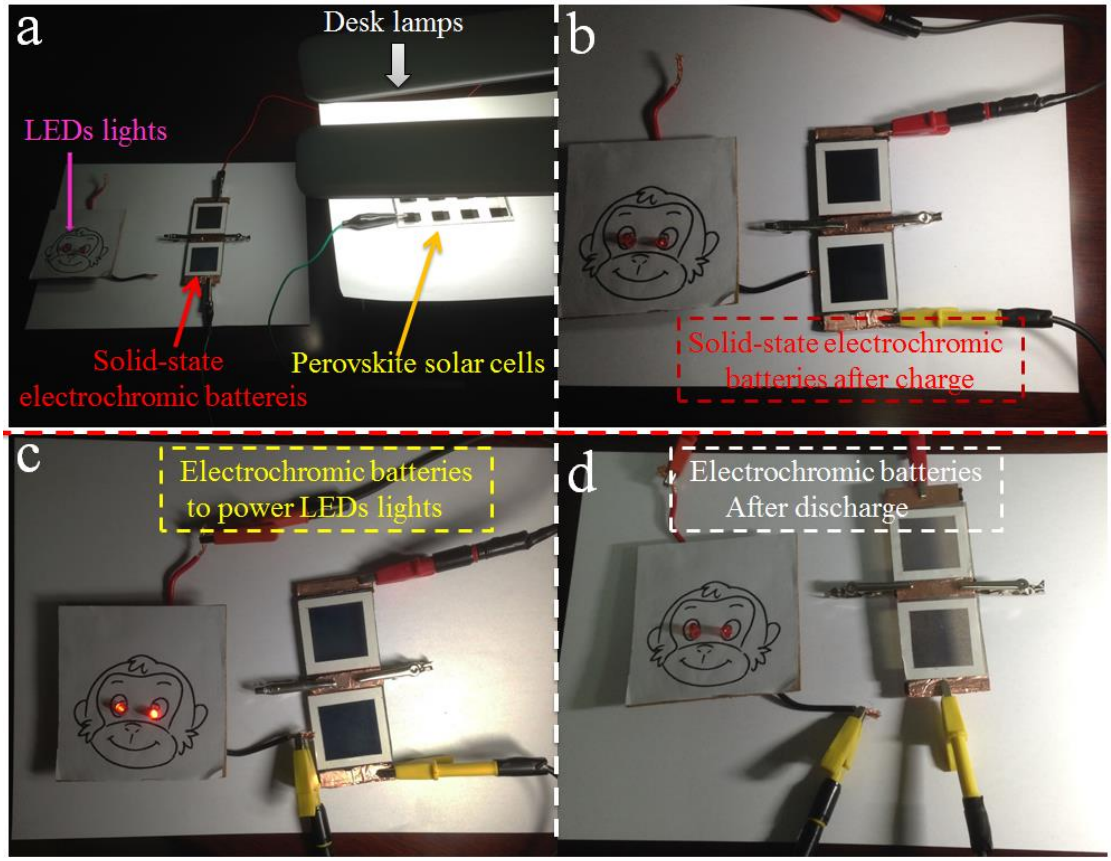

Figure S6. (a) Electrochromic batteries are charged by the perovskite solar cells under illumination of common desk lamps. (b) Electrochromic batteries in the fully charged state (blue color). (c) Electrochromic batteries as the power source to drive LEDs lights. (d) Electrochromic batteries in the fully discharged state (bleached state).

Video 1: From energy harvest to storage and reutilization. (Serial perovskite solar cells are illuminated by common desk lamps to power serial solid-state electrochromic batteries, which then to drive LEDs)

Video 2: Coloration and bleaching processes of solid-state electrochromic battery powered by perovskite solar cells under illumination of simulated sunlight.

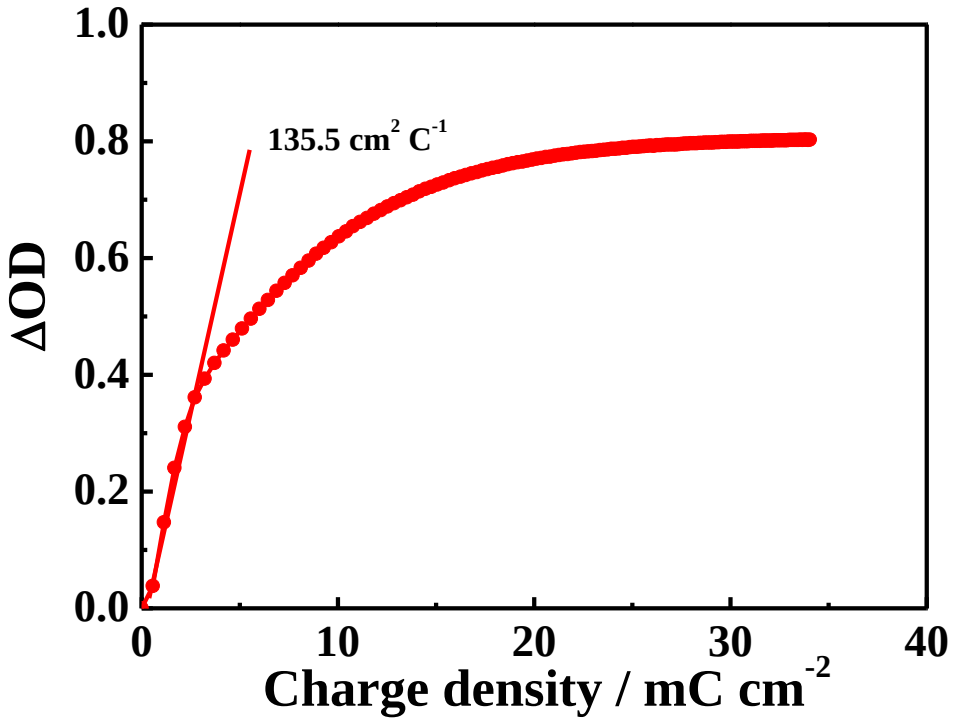

Figure S7 Variation of the in situ optical density (ΔOD) vs. charge density for the designed solid-state electrochromic batteries.

References:

1. G.-f. Cai, J.-p. Tu, J. Zhang, Y.-j. Mai, Y. Lu, C.-d. Gu and X.-l. Wang, *Nanoscale*, 2012, **4**, 5724-5730.
2. X. Xia, C. Zhu, J. Luo, Z. Zeng, C. Guan, C. F. Ng, H. Zhang and H. J. Fan, *Small*, 2014, **10**, 766-773.
3. D. Zhou, D. Xie, F. Shi, D. H. Wang, X. Ge, X. H. Xia, X. L. Wang, C. D. Gu and J. P. Tu, *J. Colloid Interface Sci.*, 2015, **460**, 200-208.
4. Z. L. Ku, Y. G. Rong, M. Xu, T. F. Liu and H. W. Han, *Sci. Rep.*, 2013, **3**, 3132.